Interaction Mechanism of U(VI) with Redox Active Covalent Organic Framework: EXAFS Spectroscopy and XPS analysis

*A. S. Helal

Nuclear materials Authority, P.O Box 540 El Maadi, Cairo, Egypt.

*Corresponding author: E-mail: ashelal@mit.edu

Abstract

Treatment of nuclear waste containing low or high level of uranium concentration is one of the critical problems in the radioactive waste management and environmental remediation. Covalent organic frameworks (COFs) are highly promising class of materials for uranium extraction due to high surface area, high stability under harsh environment and tunable structure. In this work, we investigated the interaction of uranium with highly stable redox active covalent organic framework by extended X-ray absorption fine structure spectroscopy (EXAFS) and X-ray photoelectron spectroscopy (XPS). More important, redox active COF has succeeded to reduce uranium concentration in contaminated solution from 1 ppm which 33.3 times higher than Environmental Protection Agency Limit (EPA) for uranium concentration in drinking water to less than 0.09 ppb. The obtained results make our redox active COF a promising adsorbent for uranium decontamination from aqueous solution.

Keywords: Uranium extraction; Covalent organic framework; EXAFS; XPS

1. Introduction

One of the major needs for maintain the human progress is finding a suitable source of energy capable of covering the human daily energy requirements. Presently, the fossil fuel including natural gas, coal and oil is considered the largest source of energy. But in the meantime, the combustion of this fuel results in increasing the greenhouse gas emission and short-lived climate pollutants that drive climate change. In order to meet the future energy requirement without injecting more carbon dioxide to the environment, nuclear energy considers one of the best and environmentally friendly resource of energy. Thousands of tons of oil, gas or coal can be replaced by few pounds of uranium fuel. The nuclear energy provides high energy density without by-products associated with combustion of fossil fuel [1-4]. Efficient nuclear waste treatment is the most critical issue for development of nuclear energy. Uranium is the most critical element in the nuclear fuel cycle, therefore, the purification and removal of uranium from different aqueous solutions are critically important [5-8]. To date, several techniques have been used for the separation and extraction of uranium from different aqueous streams. These include mainly solvent extraction [9-12], exchange resins [13-16], membrane-based extraction [17-18], reductive precipitation [19-20] and electrochemical extraction [21-22]. In the meantime, there are several disadvantages are facing traditional methods including chemical additions, solvent degradation, complex setup, generation of hazardous or dangerous secondary waste, multi-step procedure, and poor efficiency which control the real application of these techniques in uranium decontamination. Solid-phase extraction procedure gains a lot of attention due to affordable cost with respect to hazardous waste, easy operation, faster kinetics and high efficiency. Novel kinds of sorbents have been developed to selectively separate and extract uranium including fibers [23-24], functionalized nanomaterials [25-26] protein-based sorbent [27-28] chalcogenides [29-30] covalent organic framework [31-32] and metal organic framework [33-35]. 2D COFs is considered a gifted sorbent for uranium decontamination due to remarkable and unique structure. This study aims to investigate the mechanism of U(VI) interaction with redox active COF by using EXAFS analysis and XPS spectroscopy.

2. Experimental Section

2.1. Synthesis of β-Ketoenamine COF

β-Ketoenamine COF as shown in Fig. 1. was prepared by the reported procedure [36]. Typically, 150 mg of 1,3,5-triformylphloroglucinol (0.714 mmol) and 237 mg of p-toluidine (2.21 mmol) are dissolved in $CHCl_3$ (7 mL). Then the obtained mixture is heated to reflux for 48 hour. after cooling to room temperature, the solvent was removed in vacuum and yellow solid product was obtained.

The Environmental Protection Agency experiments was done by contact of 10 mg of the redox active COF with 30 mL of drinking water which as the accepted concentrations of Na, K, Ca and Mg spiked with 1 ppm uranium which is 33.3 time higher than the EPA limit in a stopper conical flask. The samples were agitated (at 200 rpm) for 3 h at 25 ± 1 °C. After equilibration and phase separation, the residual uranium concentration (Ceq, $mgUL^{-1}$) in the aqueous phase was determined. The uranium concentration concentrations in solution before and after adsorption was measured using Tandem Triple Quadrupole ICP-MS.
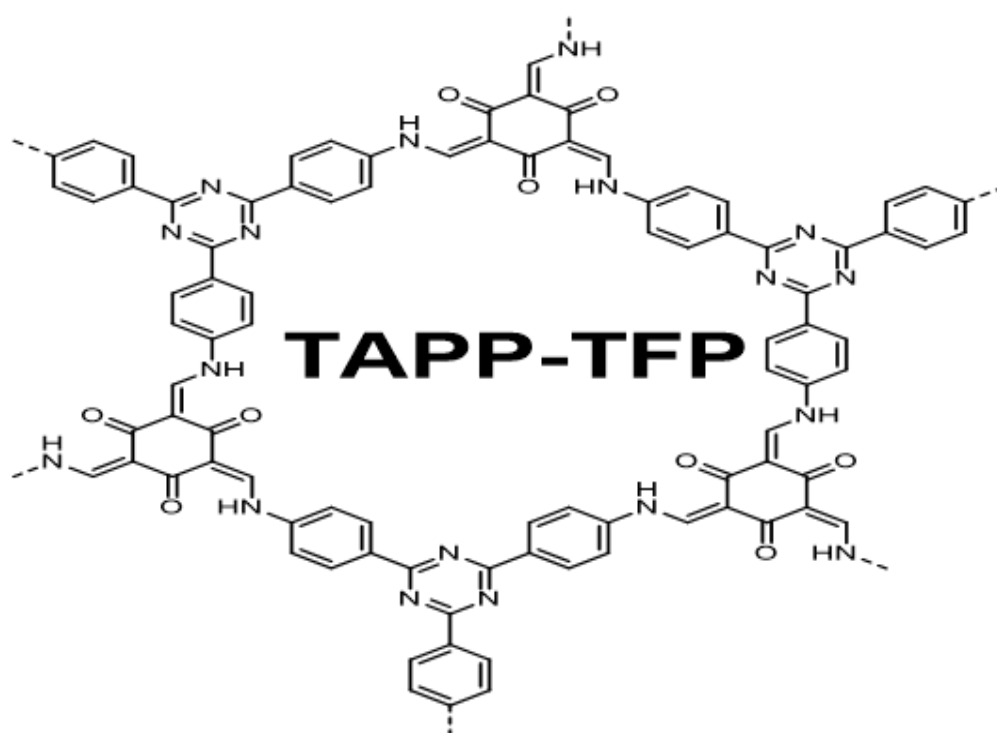
Fig. 1 The unit cell of the redox active COF used in this work.

2.2. Characterization techniques

X-ray photoelectron spectroscopy (XPS) results was measured by PHI Versaprobe II XPS, it has a C60 cluster-ion gun and a floating voltage argon single-ion gun in order to do depth profiling. The cluster-ion gun is considered nondestructive depth profiling for softer materials which can be damaged by single-ion bombardment. On the other hand, this XPS has a portable transfer vessel in order to load the processed samples into the XPS without exposure to air; an in-situ heat/cold stage (-120C to 500C); and X-ray induced secondary electron imaging (SXI), which

help in setting up for small area analysis. The samples of the solid U(VI)-loaded materials for EXAFS were prepared as required (10 mg of each sample will put in contact with 15 ml of 100 ppm uranium standard solution which adjusted at pH 6 for 180 min contact time.). After the adsorption process completed, the samples were taken to centrifuge at 10000 rpm for 30min to collect the redox active COF material. The sediments were then mounted in holes machined in Teflon sample holders, sealed with Kapton tape, and subjected to EXAFS measurements. The spectrum of

EXAFS is recorded at the U-LIII edge (17,166 eV) in fluorescence mode. The range of recording is from 17.0 to17.9 kev, by using synchrotron radiation at the beamline 1W1B of Beijing Synchrotron Radiation Facility (BSRF). The incident X-ray beam was tuned by double crystal monochromator, silicon (111) to achieve the required energies. The calibration of monochromator energy was achieved by measuring the yttrium foil (K-edge 17,038 eV) in transmission mode.

Athena software was applied to treat raw EXAFS oscillations for background subtraction, spline-fit, and normalization in order to obtain Fourier transform spectra. The atomic background function was optimized by using Rbkg 1.2 through applying the autobk utility. In order to determine the required metric parameters such as (neighboring atomic distances (R), EXAFS Debye-Waller factors ($\sigma2$) and coordination numbers (N)) from the EXAFS results. The program FEFF6 and FEFFIT code were applied to calculate and optimize the theoretical phase shift and amplitude functions for single and double scattering paths using the model structure of uranyl glutarimidedioxime [37]. Prior to analysis, the k3-weighted EXAFS spectra are Fourier transformed over a k-space range of ~3.0-14.0 Å-1. All the fitting operations are performed in R-space of ~1.0-3.5 Å.

3. Results and Discussion

3.1. EXAFS analysis

The first shell was composed exclusively of the tightly-bound uranyl axial oxygen (O_{yl}) with degeneracy fixed at 2. The second shell was composed of light scatterers at two different distances with equal, but variable degeneracy (O1, N1). The third shell was composed of light scatterers at different distances with equal, but variable degeneracy (C). ΔR and σ^2 were free parameters for all direct scattering paths. Degeneracy was a free parameter for all direct scattering paths except Oyl. Data were not fit beyond 3.5 Å in R-space due to the large noise in the data. The first shell was composed exclusively of the tightly-bound uranyl axial oxygen (O_{yl}) with degeneracy fixed at 2. The second shell was composed of light scatterers at two different distances with equal, but variable degeneracy (O1, N1). The third shell was composed of light scatterers at different distances with equal, but variable degeneracy (N2, C). ΔR and $\sigma2$

were free parameters for all direct scattering paths. Degeneracy was a free parameter for all direct scattering paths except Oyl. This model structure is most consistent with a coordination environment consisting of 2-3 chelating ligands per uranyl.

Data were not fit beyond 3.5 Å in R-space due to the large noise in the data. U complex with the N-containing groups. The *R* and *N* about C and N elements in the second and third shell confirm this mechanism. The Fourier transform is displayed on the top, with the magnitude (top) and real components. The bottom image is the artemis plot. Grey lines display the fitting window. The extracted EXAFS oscillations (up) and their corresponding FT (down) recorded on redox active COF are showed in Table 1.

3.2. XPS analysis

X-ray photoelectron spectroscopy spectra play a critical role in determining the nature of formed ligand and the oxidation state of the elements inside the material. Figure 2a shows the survey results of XPS spectra for the redox active COF before and after uranium loading. A sharp peak of binding energy (BE) of 382 eV was appeared after the uranium sorption which confirmed the binding of uranium on the COF. From Fig. 2a, a new sharp peak for N1S with binding energy has been reported after U(VI) adsorption. Moreover, the peak of O1S was shifted from 532 to 531 eV proofing the sharing of oxygen atom in the complexation of uranium. All of these results indicated that -N-U-O- bonds were formed. This was supported by the presence of peak of U4F7 after U(VI) sorption process (Fig. 2b). The main peak of U4F7 is located at about 382 eV. Both the main photoelectron peak of U4F7 and the shake-down satellite are in the range reported previously. All of these results confirming that U(VI) adsorbed onto nanochannels of the COF through pure chemical bonding.

Encouraged by the impressive interaction mechanism between U(VI) and redox active COF, we further investigated the extraction performance of the removal of uranium in spiked drinking water with a concentration of 1 mg L^{-1}, which is 33.3 times higher than the Environmental Protection Agency (EPA) limit in drinking water (30 ppb). The redox active COF has succeeded in decreasing uranium concentration in drinking water from 1 mg L^{-1} to less than 0.09 ppb within 4 h only which met the US and Egypt EPA requirement for drinking water.

Fig. 1 Data (open symbols) and best-fit model (line) for fit of EXAFS data for uranyl – Redox active COF.

Table. 1 EXAFS fits for redox active COF exposed to environmental water contaminated with uranium.

Sample	Shell	R(Å)	N	σ^2	R-factor
1 shell	U-O_y	1.80	2.0	0.0009	0.0317
2 shell	U-O	2.36	3.0	0.0016	
	U-N	2.55	3.0	0.0018	
3 shell	U-C	3.43	3.0	0.0025	
	U-N	2.95	2.8	0.0256	

Fig. 2 XPS general spectra of redox active COF: (a) XPS survey results before and after uranium loading; (b) U4f7 core-level spectrum of U-loaded redox active COF.

4. Conclusion

A series of uranyl-contacted with redox active COF were analyzed by EXAFS and XPS spectroscopy to investigate the interaction mechanism between U(VI) and the COF. Under uranium contaminated solution conditions, the model structure is most consistent with a coordination environment consisting of 2-3 chelating ligands per uranyl. Data were not fit beyond 3.5 Å in R-space due to the large noise in the data. U complex with the N-containing groups. The R and N about C and N elements in the second and third shell confirm this mechanism. The obtained XPS results confirmed that U(VI) adsorbed into the nanochannels of the COF through pure chemical bonding. Moreover, the redox active COF succeeded in removing uranium from spiked drinking water to less than the EPA uranium limit for drinking water (30 ppb). All of these findings make a redox active COF a promising technology for uranium decontamination from drinking water, ground water and nuclear waste.

References

[1] M. Kaur, H. Zhang, L. Martin, T. Todd, Y. Qiang, Environ. Sci. Technol. 2013, 47, 11942−11959.

[2] P.A. Kharecha, J.E. Hansen, Environ. Sci. Technol. 2013, 47, 4889−4895.

[3] A. Markandya, P. Wilkinson, The Lancet 2007, 370, 979−990.

[4] F. Lewis, M. Hudson, L. Harwood, Synlett 2011, 2011, 2609−2632.

[5] X. Sun, H. Luo, S. Dai, Chem. Rev. 2012, 112, 2100–2128.

[6] Loveland, W. D.; Morrissey, D. J.; Seaborg, G. T. Modern Nuclear Chemistry; Wiley-Interscience: Hoboken, NJ, 2006.

[7] Choppin, G. R.; Khankhasayev, M. K. Chemical Separation Technologies and Related Methods of Nuclear Waste Management: Applications, Problems, and Research Needs; Kluwer Academic Publisher: Dordrecht, The Netherlands, 1999.

[8] Lan Ling and Wei-xian Zhang. J. Am. Chem. Soc. 2015, 137, 2788−2791

[9] M. Tan, C. Huang, S. Ding, F. Li, Q. Li, L. Zhang, C. Liu, S. Li, Separation and Purification Technology, 2015, 146, 192–198.

[10] A. Rout, K.A. Venkatesan, T.G. Srinivasan, P.R. Vasudeva Rao, Journal of Hazardous Materials, 2012, 221–222, 62-67.

[11] T.A. Lasheen, M.E. Ibrahim, H.B. Hassib, A.S. Helal, Hydrometallurgy, 2014, 146, 175–182.

[12] M.E. Ibrahim, T.A. Lasheen, H.B. Hassib, A.S. Helal, Journal of Dispersion Science and Technology, 2014, 35, 599-606.

[13] R. Ruhela, N. Iyer, M. Yadav, A.K. Singh, R.C. Hubli, J.K. Chakravartty, Green Chem., 2015, 17, 827-830.

[14] A.C. Sather, O.B. Berryman, J.R. Jr, Chem. Sci. 2013, 4, 3601 – 3605.

[15] J. Qian, S. Zhang, Y. Zhou, P. Dong, D. Hua, RSC Adv. 2015, 5, 4153-4161.

[16] C. Gunathilake, J. Górka, S. Dai, M. Jaroniec, J. Mater. Chem. A, 2015, 3, 11650-11659.

[17] S.D. Kolev, A.M. St John, R.W. Cattrall, Journal of Membrane Science, 2013, 425–426, 169-175.

[18] S. Panja, P.K. Mohapatra, S.C. Tripathi, P.M. Gandhi, P. Janardan, Journal of Hazardous Materials, 2012, 237–238, 339-346.

[19] I. Doroshenko, J. Zurkova, Z. Moravec, P. Bezdicka, J. Pinkas, Ultrasonics Sonochemistry, 2015, 26, 157-162.

[20] G.I. Bouala, N. Clavier, R. Podor, J. Cambedouzou, A. Mesbah, H.P. Brau, J. Léchelle, N. Dacheux, CrystEngComm, 2014, 16, 6944-6954.

[21] Y. Lio, M. Wang, D. Chen, Applied Surface Science, 2019, 484, 83-96.

[22] C. Liu, P. Hsu, J. Xie, J. Zhao, T. Wu, H. Wang, W. Liu, J. Zhang, S. Chu, Y. Cui. Nature Energy 2017, 2, 17007.

[23] D. Wang, J. Song, J. Wen, Y. Yuan, Z. Liu, S. Lin, H. Wang, H. Wang, S. Zhao, X. Zhao, M. Fang, M. Lei, B. Li, N. Wang, X. Wang, H. Wu, Adv. Energy Mater. 2018, 8, 1802607.

[24] Xiao Xu, H. Zhang, J Ao, L. Xu, X. Liu, X. Guo, J. Li, L. Zhang, Q. Li, X. Zhao, B. Ye, D. Wang, F. Shend, H. Ma, Energy Environ. Sci., 2019, 12, 1979-1988.

[25] A. S. Helal, E. Mazario, A. Mayoral, P. Decorse, R. Losno, C. Lion, S. Ammar, M. Hémadi. Environ. Sci.: Nano, 2018, 5, 158-168.

[26] Q. Sun, B. Aguila, J. Perman, A. S. Ivanov, V. S. Bryantsev, L. D. Earl, C. W. Abney, L. Wojtas, S. Ma, Nature Communications, 2018, 9, 1644.

[27] L. Zhou, M. Bosscher, C. Zhang, S. O¨zçubukçu, L. Zhang, W. Zhang, C. J. Li, J. Liu, M. P. Jensen and L. Lai, Nat. Chem., 2014, 6, 236.

[28] S. O. Odoh, G. D. Bondarevsky, J. Karpus, Q. Cui, C. He, R. Spezia, L. Gagliardi. J. Am. Chem. Soc. 2014, 136, 17484−17494.

[29] M. Feng, D. Sarma, X. Qi, K. Du, X. Huang, M. G. Kanatzidis. J. Am. Chem. Soc. 2016, 138, 12578−12585.

[30] M. Feng, D. Sarma, Y. Gao, X. Qi, W. Li, X. Huang, M. G. Kanatzidis. J. Am. Chem. Soc. 2018, 140, 11133−11140.

[31] Q. Sun, B. Aguila, L. D. Earl, C. W. Abney, L. Wojtas, P. K. Thallapally, S. Ma. Adv. Mater. 2018, 30, 1705479.

[32] X. H. Xiong, Z. W. Yu, L. L. Gong, Y. Tao, Z. Gao, L. Wang, W. H. Yin, L. X. Yang, F. Luo. Adv. Sci. 2019, 1900547.

[33] L. Xu, D. Zhang, F. Ma, J. Zhang, A. Khayambashi, Y. Cai, L. Chen, C. Xiao, S. Wang. ACS Appl. Mater. Interfaces 2019, 11, 21619−21626.

[34] R. Liu, Z. Wang, Q. Liu, F. Luo, Y. Wang. Eur. J. Inorg. Chem. 2019, 735–739.

[35] W. Liu, Y. Wang, L. Song, M. A. Silver, J. Xie, L. Zhang, L. Chen, J. Diwu, Z. Chai, S. Wang, Talanta 2019, 196, 515–522.

[36] C. R. DeBlase, K. E. Silberstein, T. Truong, H. D. Abruña, W. R. Dichtel. Journal of American Chemical Society 2013, 135, 45, 16821–16824.

[37] C. W. Abney, R.T. Mayes, M. Piechowica, Z. Lin , V.S. Btryantsev, G.M. Veith, S. Dai, W. Lin. Energy Environmental Science, 2016, 9(2), 448-453.